ANALYSIS OF SINGLE STRAP HYBRID BUTT JOINT IN LAMINATED FRP COMPOSITES

[1] Dr. M. Sivakumar, [2]Dr. V. Venugopal, [3]Dr. G. Mahesh, [4]Dr. A.K.S. Ansari,
[1]Professor, Dept. of Mechanical Engineering, Malla Reddy College of Engineering, Sec-100
[2] Professor, Department of Mechanical Engineering, Malla Reddy College of Engineering, Sec-100
[3] Associate Professor, Department of Mechanical Engineering, Malla Reddy College of Engineering, Sec-100
[4] Professor,Department of Mechanical Engineering, Malla Reddy College of Engineering, Sec-100

Abstract— The present investigation deals with the static analysis of adhesively bonded single strap hybrid butt joint in laminated FRP composites using three-dimensional theory of elasticity based finite element method. The finite element model is validated and is extended for the analysis of a single strap hybrid butt joint made of generally and specially orthotropic laminates subjected to longitudinal load with C-F end condition. The stresses are computed in adherends and adhesive. The results of the present analysis reveals that the three-dimensional stress analysis is required for the analysis of single strap hybrid butt joint in laminated FRP composites.

Index terms: SSHBJ, FEM, FRP, C-F

1. INTRODUCTION

Fiber reinforced plastic (FRP) materials have proven to be very successful in structural applications. They are widely used in the aerospace, automotive and marine industries. FRP materials or composites behave differently than typical metals such as steel or aluminum. A typical composite contains layers of aligned fibers oriented at different angles held together by a resin matrix, giving high strength and stiffness in different directions. This anisotropy can cause difficulties when joining two parts together, especially if the two pieces have different stiffness and strength characteristics. The joint can potentially become the weakest link in the structure due to the large amount of load it must transfer. There are wide varieties of ways to join different parts together. Two major methods include mechanical fastening and adhesive bonding. Adhesive bonding of structures has significant advantages over conventional fastening systems. Bonded joints are considerably more fatigue resistant than mechanically fastenedstructures because of the absence of stress concentrations that occur at fasteners. Joints may be lighter due to the

Roy et.al (4) employed shear specimens and butt-joint specimens to measure the shear and tensile strengths of five types of adhesive bonds for brittle and Homalite polymers. In order to examine the possible stress singularities, they have employed two optical techniques, photo elasticity and coherent gradient sensing to record fringe pattern until specimens failed.

2. PROBLEM MODELING

2.1 Geometry.

The geometry of the single strap hybrid butt joint used for the validation is as shown in Fig.1. Where the dimensions are taken as t =20 mm, t1=5 mm, t2 = 5 mm, t3 = 2 mm, l = 100 mm . The width of the plate in the Z-direction is taken as 25 mm.

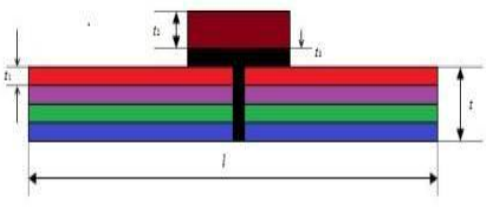

ISSN (PRINT): 2393-8374, (ONLINE): 2394-0697, VOLUME-5, ISSUE-1, 2018
DOI: 10.21276/ijcesr.2018.5.1.34

All dimensions are in mm Fig. 1 Geometry of the single strap hybrid butt joint

2.2 Finite Element Model

The finite element mesh is generated using a three-dimensional brick element 'SOLID 45' of ANSYS

[8]. This element (Fig. 2) is a structural solid element designed based on three-dimensional elasticity theory and is used to model thick orthotropic solids. The element is defined by 8

nodes having three degrees of freedom per node: translations in the nodal x, y, and z directions.

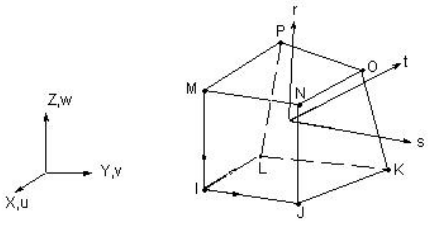

Fig. 2 SOLID 45 Element

2.3 Loading

The following types of loads are applied for validation and prediction of the response of the structure for the present analysis.

i)A longitudinal uniform pressure of 10MPa is applied for the validation purpose

ii)A uniform longitudinal load of 10 MPa is applied for the present analysis

2.4 Boundary Conditions

one end of the joint is clamped and the other end is restricted to move in the transverse direction (C-F). A uniform longitudinal load of 10 MPa is applied.

2.5 Material Properties

The following mechanical properties are used for the validation and analysis of single strap hybrid butt joint (7).

i) Graphite/epoxy FRP (adherend) EL = 172.72 GPa; ET = 6.909 GPa; νLT = νLZ = 0.25;

GLT = 3.45 GPa; GTT = 1.38 Gpa

ii) Epoxy (adhesive)
E = 5.171 GPa; ν = 0.35
iii) Strap
E = 200 GPa; ν = 0.25

2.6 Laminate sequence

i) Two +θ0/-θ 0/-θ 0/+θ 0 laminated FRP composite plates are used as adherends for the present analysis. The value of θ is measured from the longitudinal direction of the structure (x-axis) and varied from 00 to 900 in steps of 150.

3. RESULTS

3.1 Validation

Fig. 3 Shows Finite element mesh on the overlap region of the single strap hybrid butt joint.

The finite element mesh divisions on the non-overlap region are same as that given for overlap region across thickness, but along the length a course mesh is considered to limit the number of nodes without loosing the accuracy of the solution. Table3. 1 shows the values of the stresses at the free surfaces where the stresses should be zero and close agreement is found. Later this model is used for the analysis of single strap hybrid butt joint made of specially and generally orthotropic laminates subjected to longitudinal loading.

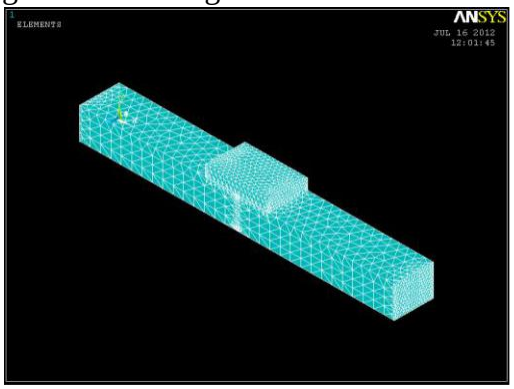

ISSN (PRINT): 2393-8374, (ONLINE): 2394-0697, VOLUME-5, ISSUE-1, 2018
DOI: 10.21276/ijcesr.2018.5.1.34

Fig. 3 Finite element mesh on the overlap region of the single strap hybrid butt joint

Table 1. values of the stresses at the free surfaces where the stresses should be zero.

NODE NUMER	STRESS IN MPA		
1393	-0.0299	-0.133	0.025
1451	0.043	-0.12	-0.008
1526	0.04779	0.0945	-0.0772
1469	0.11365	-0.405	-0.0485
1493	-0.1251	-0.0801	0.053
1475	-0.0886	0.0175	0.023
1422	-0.0704	-0.4421	-0.0536
1444	0.0128	0.0853	0.0782
1432	0.06672	-0.19424	0.0465
1462	0.0314	0.1223	0.0186

3.2Variation of maximum stresses in the

Laminates with respect to the fiber angle θ:

The variation of stresses is due to the variation in internal stiffness in the adherends due to the change in fiber angle. The inter laminar effects at the interfaces of adherends also influences the stresses.

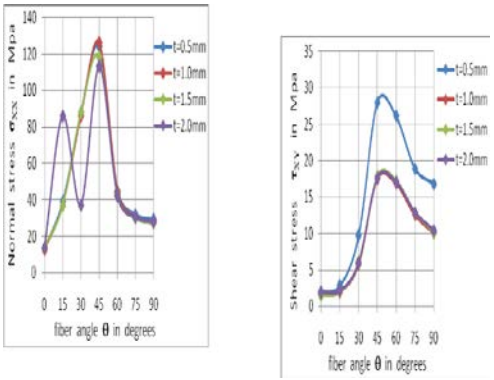

Fig.4 Variation of σxx in the Laminate

This Fig shows that the stress increases Fig. 7 Variation of τxy in the Laminate with increase in fiber angle θ upto 45˚ and decreases

with increase in angle. For the adhesive thickness t=2.0 mm the stress increases upto 15˚ and decreases with increase in angle. The maximum stress is at 45˚ and minimum stress is at 0˚ for all adhesive thicknesses.

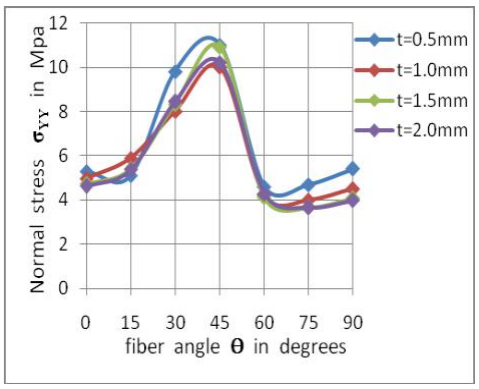

Fig. 5 Variation of σyy in the Laminate

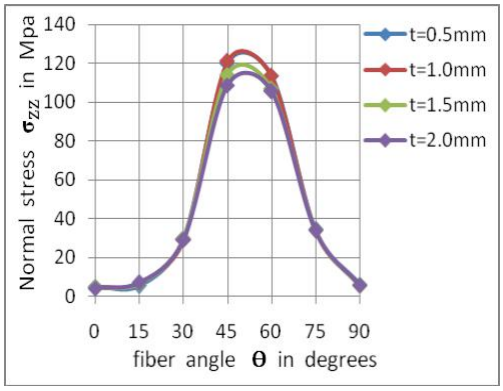

Fig. 6 Variation of σzz in the Laminate

Fig.5 and 6 shows that the stress value is low

between 0 to 15˚ and gradually increases upto 45˚

where the stress is maximum. Thereby it is followed

with decrease in stress value with increase in fiber

angle. The minimum stress value is found to be at

75˚. The induced stress is very low in magnitude for

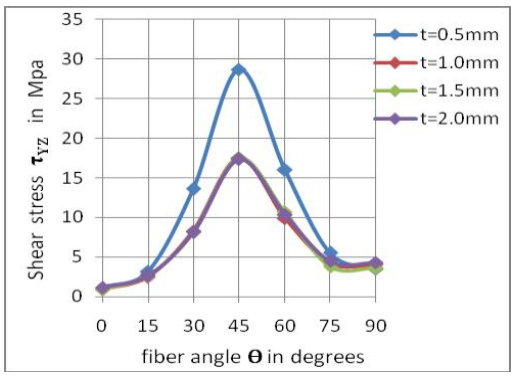

ISSN (PRINT): 2393-8374, (ONLINE): 2394-0697, VOLUME-5, ISSUE-1, 2018
DOI: 10.21276/ijcesr.2018.5.1.34

Fig. 8 Variation of τxy in the Laminate with

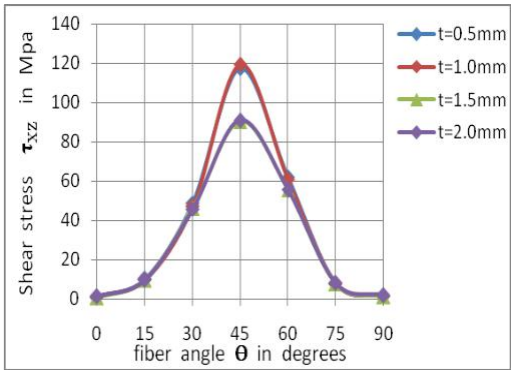

Fig.9 Variation of τzx in the Laminate Fig.7, 8 and 9 depicts the variation of shear stress τxy, τyz and τxz with respect to fiber angle θ. The induced shear stress is observed to be maximum at 45˚ and minimum in between 0 to 15˚. The stress is high for thickness t=0.5mm

Fig.10 Variation of δx in the Laminate

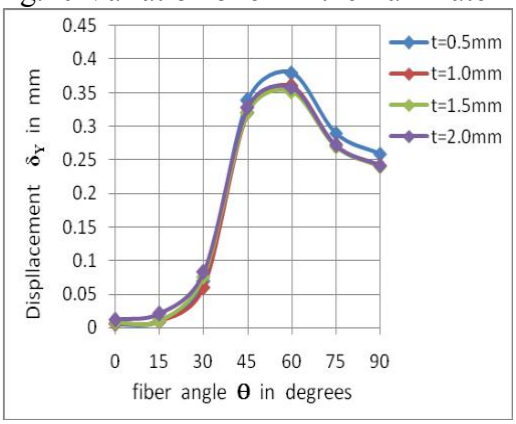

Fig. 11 Variation of δy in the Laminate Fig.10 and 11 shows the variation of displacement δx and δy with respect to fiber angle θ. The curve gradually increases with increase in angle and the displacement is observed to be maximum at 60˚ followed by decrease in value with increase in angle. The stress is minimum at 0˚.

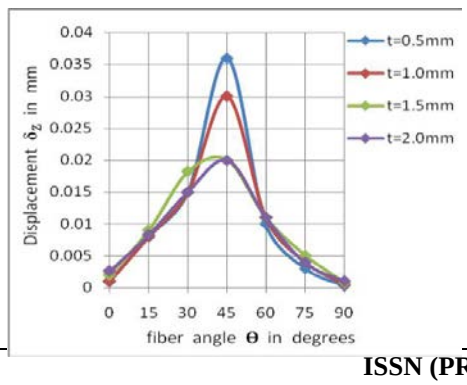

Fig. 12 Variation of δz in the Laminate

Fig. 12 depicts the variation of displacement δz with respect to fiber angle θ. The displacement increases with increase in fiber angle upto 45˚ and thereby it decreases with increase in angle. The maximum displacement is more for adhesive thickness t=0.5mm when compared to other thicknesses.

3.3Variation of maximum stresses in the Vertical Adhesive with respect to the fiber angle θ:

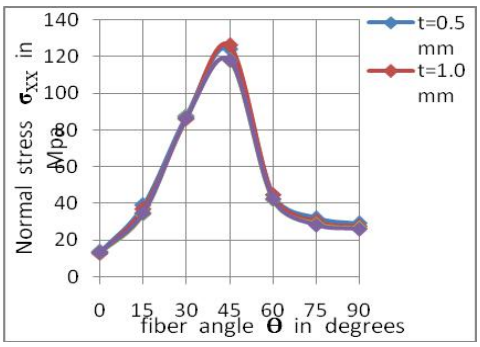

Fig. 13 Variation of σxx in the adhesive

This fig. shows that with increase in fiber angle θ the stress also increases and is maximum at 45˚ and decreases with increase in angle.

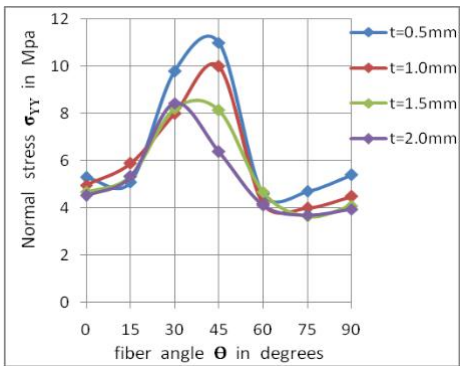

Fig. 14 Variation of σyy in the adhesive

ISSN (PRINT): 2393-8374, (ONLINE): 2394-0697, VOLUME-5, ISSUE-1, 2018
DOI: 10.21276/ijcesr.2018.5.1.34

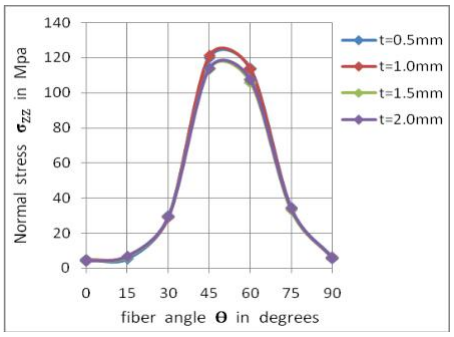

Fig. 15 Variation of σzz in the adhesive

Fig. 14 and 15 depicts the variation that stress increases with increase in fiber angle θ. The maximum stress is observed to be at an angle of 45˚. The induced stress is maximum for the adhesive thickness t=0.5mm.

Fig. 16 Variation of τxy in the adhesive

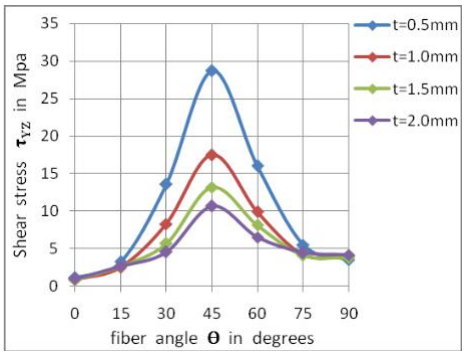

Fig. 17 Variation of τyz in the adhesive

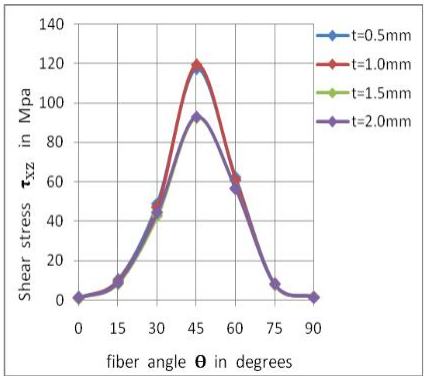

Fig. 18 Variation of τzx in the adhesive

Fig. 16,17 and 18 shows the variation of shear stress τxy, τyz and τxz with respect to fiber angle θ. The shear stress is minimum at 0˚ and increases with increase in angle. The shear stress is observed to be maximum at an angle of 45˚ and decreases with increase in angle. The induced shear stress is minimum for the adhesive thickness t=2.0mm when compared to other thicknesses.

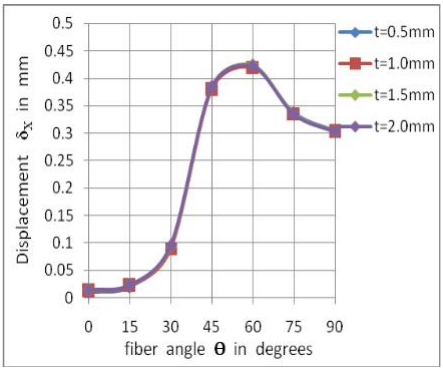

Fig. 19 Variation of δx in the adhesive

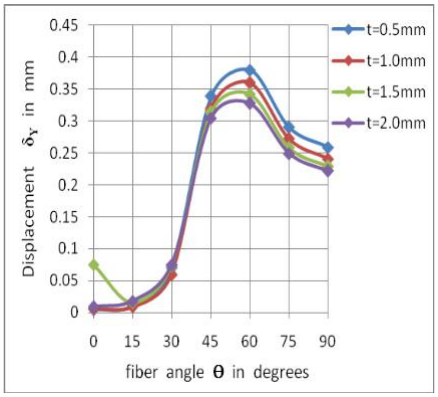

Fig. 20 Variation of δy in the adhesive

This Fig.depicts the variation of displacement δx and δy with respect to fiber angle θ. The displacement increases with increase in fiber angle followed by decrease in value with increase in angle. The displacement is maximum at 60˚.

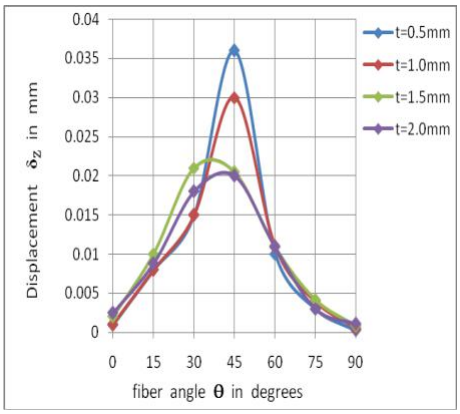

Fig. 21 Variation of δz in the adhesive This fig shows that the displacement is maximum at 45˚ and minimum at 0 and 90˚. The maximum displacement decreases with increase in all adhesive thickness.

3.4 Variation of maximum stresses in the Horizontal Adhesive with respect to the fiber angle θ:

ISSN (PRINT): 2393-8374, (ONLINE): 2394-0697, VOLUME-5, ISSUE-1, 2018
DOI: 10.21276/ijcesr.2018.5.1.34

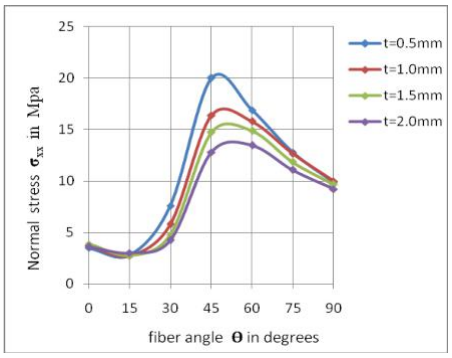

Fig. 22 Variation of σxx in the adhesive

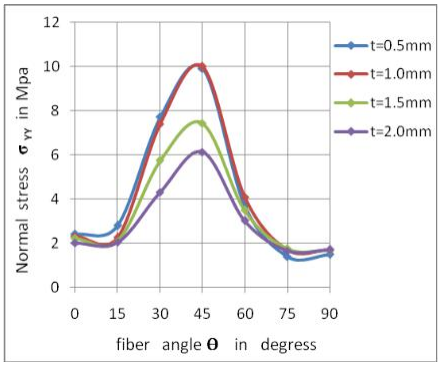

Fig.23 Variation of σyy in the adhesive

Fig. 22 and 23 depicts the variation of Normal stress σxx and σyy with respect to fiber angle θ. The stress increases with increase in fiber angle θ followed by decrease with increase in angle.The stress is maximum at 45˚ and minimum in between 0 to 15˚.

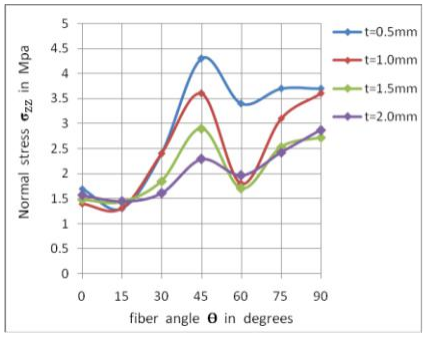

Fig.24 Variation of σzz in the adhesive

This Fig.shows that the stress increases with increase in fiber angle θ upto 45˚ and decreases upto 60˚ followed by increase with increase in angle. The induced stress is maximum for the adhesive thickness t=0.5mm.

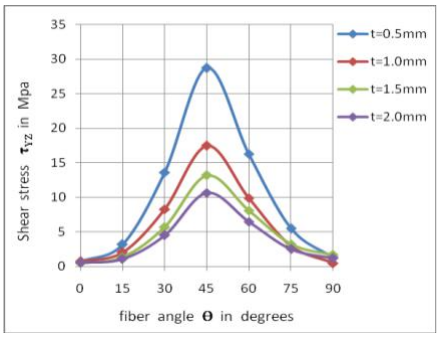

Fig.25 Variation of τxy in the adhesive

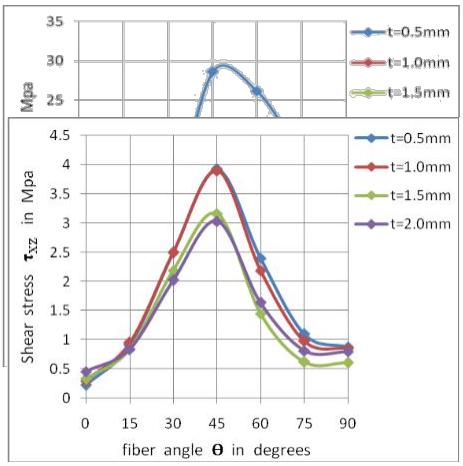

Fig.26 Variation of τyz in the adhesive

Fig.27 Variation of τzx in the adhesive

Fig. 25, 26 and 27 shows the variation of shear stress τxy, τyz and τxz with respect to fiber angle θ.The induced shear stress is maximum at 45˚ and minimum in between 0 to 15˚ and 75 to 90˚. The induced shear stress is minimum for the adhesive thickness t=2.0mm

ISSN (PRINT): 2393-8374, (ONLINE): 2394-0697, VOLUME-5, ISSUE-1, 2018
DOI: 10.21276/ijcesr.2018.5.1.34

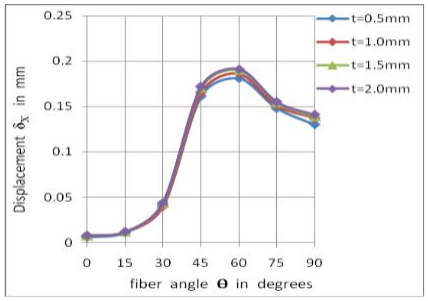

Fig.28 Variation of δx in the j adhesive

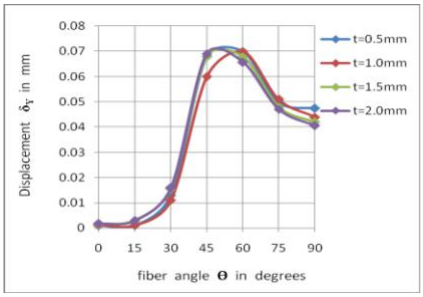

Fig.29 Variation of δy in the adhesive

Fig.28 and 29 shows the variation of displacement δx and δy with respect to fiber angle θ. The displacement increases with increase in fiber angle followed by decrease in value with increase in angle. The maximum displacement is at an angle 60˚ and minimum at 0˚.

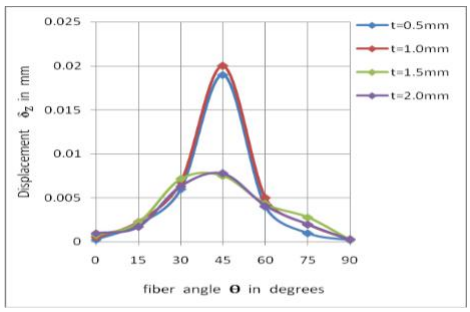

Fig.30 Variation of δz in the adhesive

Fig.30 shows the variation of displacement δz with respect to fiber angle θ. The displacement is maximum at 45˚ and minimum at 0 and 90˚. The maximum displacements are observed to be more for the adhesive thickness t=1.0mm

4. CONCLUSIONS:

Three-dimensional finite element analysis has been taken up for the evaluation of the stresses in the adherends and adhesive of single strap hybrid butt joint made of FRP laminates of generally and specially orthotropic nature subjected to longitudinal load with C-F end conditions. The following conclusions are drawn:

☐ The normal stresses σ xx and σ zz in laminate and vertical adhesive are very high in magnitude between 30˚ and 55˚. The fiber angle range i.e., 0˚-15˚ and 75˚-90˚ is recommended in order to avoid the failure of fibers due to tearing or substrate failure.

☐ The displacements in adherends and adhesive are observed to be almost same and minimum between the fiber angles 0˚ and 15˚.

☐ Maximum value of τ xz is found in vertical adhesive for longitudinal loading. Hence interfacial failure between the adhesive and the adherend or cohesive failure may likely to occur. This stress is observed to be minimum between 0 ˚-15˚ and 75˚-90˚. Fiber angle orientation 0°-15° or 75°-90° is preferable to avoid the interfacial failure and cohesive failure.

• Magnitude of all the stresses is very less in the horizontal adhesive when the structure is subjected to longitudinal loading

• Variation of the stresses in the width direction is significant and therefore three-dimensional analysis is necessary.

REFERENCES

1. Reedy, E.D., and Guess, T.R., 'Interface corner stress states: plasticity effects', Int. journal of Fracture, V.81, No.3, 1996, p269-282.

2. Reedy,E.D.,andGuess,T.R.,

'Comparison of butt tensile strength data with interface corner stress intensity factor prediction',

Int. J. Solids& Structures, 30, 1993, 2929.

3. Reedy, E.D., and Guess, T.R., 'Interface corner failure analysis of joint strength: Effect of

Adherend Stiffness', Int. J. of Fracture, V.88, 4,
1993, p305-314.

4. Roy Xu, L., Sreeparna Sengupta., and

Huacheng Kuai., 'An experimental and numerical investigation of adhesive bonding strengths of

polymer materials', International Journal of Adhesion & Adhesives, 24, 2004, p455-460.

5. Fassio, F., Santini, S., and Vallee, T.,

'Tensile tests on bonded double strap joints between pultruded GFRP profiles', Proceedings of the international symposium on bond behaviour of FRP in structures, (BBFS 2005).

6. Mitra, A.K., and Ghosh, B., 'Interfacial stresses and deformations of an adhesive bonded double strap butt joint under tension', computers

&structures V.55, 4, 1995, p687-694.

7. Tungikar, V.B., and Rao, K.M., 'Three dimensional exact solution of thermal stresses in rectangular composite laminate', Composite

Structures, 27, 1994, p419-430.

8 .ANSYS reference manuals (2006)

9. Mallick,P.K., 'Fiber-reinforced Composites', MARCEL DEKKER, INC,

1988, P159-162.

10. Jones, R.M., 'Mechanics of Composite Material', Scripta book company,

Wasington D.C, 1975.

11. Isaac, M.D., and Ishai Ori., 'Engineering Mechanics of Composite Materials',

Oxford University Press, 1994.